Journal of Photochemistry, 8 (1978) 307 - 319

ABSOLUTE QUANTUM YIELDS OF CO FOR SELECTED-STATE PHOTODISSOCIATION

G. H. ATKINSON, M. E. McILWAIN, C. G. VENKATESH and D. M. CHAPMAN
Department of Chemistry, Syracuse University, Syracuse, N. Y. 13210 (U.S.A.)
(Received August 4, 1977; in revised form November 4, 1977)

Summary

Experimental techniques designed to measure the absolute quantum yield of a gas phase photochemical product following selected-state laser excitation of the parent molecule are described. Specifically, measurements of both product yields at millitorr pressures and absorption coefficients for discretely (1.0 nm bandwidth) absorbing low pressure samples over narrow (0.02 nm) spectral regions are presented. Data for the production of CO from a single vibronic level in glyoxal are used to characterize the capabilities and limitations of the entire experimental approach.

1. Introduction

The pathway and efficiency by which polyatomic molecules dissociate in the gas phase can be dramatically influenced by the rovibronic characteristics of the excited state(s) in which they are initially populated [1 - 6]. An understanding of this dependence, as well as the mechanism(s) underlying it, is a fundamental step in the design of experiments which use narrow bandwidth tunable radiation to control dissociative reactions through the selection of excited state populations. In spite of the resurgence of interest in state-selected chemistry brought about by the expanding capabilities of tunable lasers and the emergence of laser-oriented isotope separation, very few data of this type are available.

The absolute quantum yield of a product following selected-state excitation is an especially useful characterization of a dissociation because it monitors the efficiency of the overall reaction. It is composed of two separate absolute measurements: (1) the number of product molecules and (2) the number of parental molecules initially in a specific excited state. The scarcity of these types of data originates, at least in part, from the difficulty and number of absolute measurements involved. For example, the product analysis must generally be carried out on very low concentrations and for only one member of a multicomponent system. Excited state concentrations

are obtained in part from the absolute absorption coefficients of the parent. In this case, the narrow bandwidth of the excitation relative to the discrete absorption bands of the parent causes the absorptivity of the sample to change rapidly over small wavelength regions. The measurements are further complicated by the small absolute absorptivity of low pressure samples and the need to correlate the absorption coefficients and product concentrations for precisely the same excitation wavelength.

In this paper we address these problems by describing experimental techniques which have been successfully used to measure the absolute quantum yields for a dissociation product as a function of the rovibronic level initially populated in the parent. Results will be presented for the absolute quantum yields of CO (ϕ(CO)) following single vibronic level (SVL) excitation of low pressure glyoxal. The emphasis of this paper is placed on the experimental techniques used to obtain ϕ(CO) values with glyoxal serving as an example. Results specifically concerning the SVL photodissociation mechanism in glyoxal leading to CO formation are presented elsewhere [6].

2. Experimental

2.1. CO concentrations

The experimental apparatus used to measure CO concentrations is shown in Fig. 1. Vacuum ultraviolet (VUV) resonance emission was used to

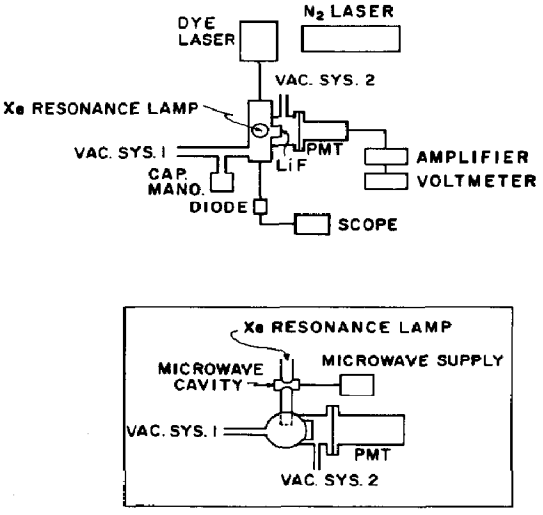

Fig. 1. Apparatus for SVL photolysis and the detection of CO by resonance emission. A nitrogen-laser-pumped dye laser generates tunable photolysis radiation with a 0.02 nm bandwidth and a 10 - 14 ns pulse duration. It passes unfocused (see footnote on p. 311) through a 10 cm long cell and onto a calibrated photodiode used to obtain intensity measurements. A microwave-driven discharge in xenon and CO is positioned perpendicular to the axis defined by the laser beam. The VUV emission passes through a LiF window and into a second vacuum chamber containing a photomultiplier with a CsI cathode. The photomultiplier signal is amplified and offset (see Fig. 2) prior to being read on a voltmeter.

monitor CO. A sealed xenon lamp powered by a 2450 MHz microwave cavity (Evenson–Broida design) produces a series of emission lines including the 147 nm resonance line of xenon. The gas mixture for the lamp consisted of 1 Torr xenon (Airco Products) and approximately 10 mTorr CO (Airco Products). The lamp body, following the design of ref. 7, was made of Pyrex and was sealed with a LiF window. No gettering material was used.

A part of the VUV lamp radiation is absorbed by CO in the reaction cell and re-emitted as resonance fluorescence [8]. The CO fluorescence was detected by a solar blind photomultiplier using a CsI cathode (EMI, Model G26E3-15, operated at a gain of 10^5). The photomultiplier was positioned perpendicular to the lamp in a chamber connected to a vacuum system completely separate from the reaction cell (insert, Fig. 1). This separation removed the potential for contamination of the MgF window of the photomultiplier by photolysis products (*e.g.* polymerization products). The two vacuum chambers were connected by a LiF window (1/16 in thick) which was transparent to the CO fluorescence.

In addition to the CsI photomultiplier, the detection system consisted of a transresistance amplifier (Fig. 2(a)) and a low pass filter (Fig. 2(b)). The transresistance amplifier is physically small to facilitate a direct connection to the photomultiplier via a TNC to BNC adapter. This reduces the susceptibility of the signal to the noise created by the discharge of a nearby nitrogen laser. The resulting gain of 3×10^9 V A^{-1} amplifies signal variations of the order of 10^{-12} A to a level of a few millivolts. The detection system also employs a current summing capability for suppressing an anode current of about 10^{-9} A due to scattered lamp radiation. The operational amplifier (Teledyne Philbrick 142902) was chosen for its low input bias current (10^{-13} A), high input impedance (10^{13} Ω) and low noise current (4×10^{-14} A peak-to-peak) at low frequencies. The filter is of a two-pole low pass type with a corner frequency of 0.6 Hz and unity gain in the passband. In operation, a 6 V output due to scattered light can be suppressed to a level whereby signal variations of less than 5 mV can be monitored. The total drift of the system was less than 1% for these conditions. The signal due to CO resonance emission was read on a voltmeter (Keithley model 150B).

Extreme care in stabilizing the lamp output was necessitated by the high amplification levels and the inherent instability of the microwave discharge. For example, the ratio of signal (CO resonance emission) to scattered light observed by the photomultiplier was as low as 10^{-4}. This meant that the intensity of the lamp had to remain constant to within 0.01% if meaningful measurements were to be made. Since commercial microwave power generators are typically regulated at 1%, additional regulation circuitry was required (Fig. 2(c)). An operational amplifier (LM308) was used as a comparator to drive the grids of a dual triode (6BL7) and thereby to regulate the current changes in the tube conductance. The hybrid circuit was suggested by the presence of the 6BL7 triode in the original microwave power supply (Raytheon Model PGM-10). In operation, the desired current is set by the ten-turn potentiometer while the plate voltage of the 6BL7 is

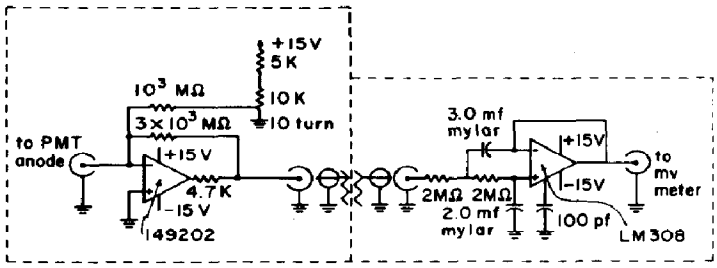

(a) (b)

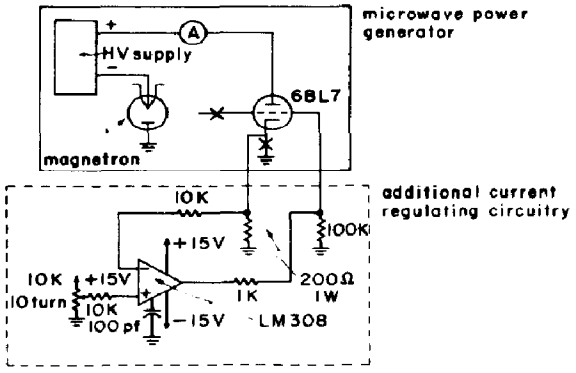

(c)

Fig. 2. (a) Signal amplifier. A signal amplifier is connected directly to the anode of an EMI G26E3-15 photomultiplier. It provides an output of a few millivolts while suppressing the contributions to the signal made by the photomultiplier dark current and scattered light. (b) Low pass filter. The system noise above 0.6 Hz is attenuated by this two-pole low pass filter. (c) Microwave power generator (Raytheon PGM-10X2) with current stabilization. Only a portion of the original pulsing circuit in a standard microwave power generator is utilized. The points at which this circuit was broken and reconnected to the regulating electronics are indicated by the symbol ×. Both triodes in the 6BL7 are placed in parallel with a total current adjustable from 0 to 100 mA. The current-comparing circuitry was added to obtain the required 0.01% regulation.

maintained at 100 V by the Variac present on the original power supply. At a typical operating current of 25 mA (about 20% of full power) and after a 5 min warm-up period, no current drift was detected within the 0.01% resolution of our instrumentation. Careful air cooling of the microwave discharge region in the lamp also minimized fluctuations. Without these stabilization measures, it would be very difficult to maintain the constant level of VUV output needed to carry out quantum yield measurements requiring more than a few seconds to complete. This type of long term stability distinguishes this application of VUV resonance emission from its use in reaction kinetics [9] and as a photochemical source [10].

The procedure for measuring the absolute number of CO molecules involved several steps. The photolysis was performed by the unfocused† output of a nitrogen-laser-pumped dye laser in a cylindrical cell of dimensions 10 cm × 2.5 cm sealed with quartz windows and having a volume of approximately 60 cm^3. The exact volume of a photolysis cell was measured by volume expansion methods. The total amount of photolysis was kept well below 5% and in all cases did not result in more than 20 mTorr of CO. The resonance lamp was not operated during the laser photolysis.

Following excitation, the contents of the photolysis cell were exposed to a trap at liquid nitrogen temperature. A variety of experimental tests were performed to establish that all detectable amounts of glyoxal as well as any products (*e.g.* formaldehyde) which could subsequently be photolyzed to CO were removed by trapping without removing CO itself. Two such tests are noteworthy.

(1) The xenon resonance lamp itself was of course capable of very efficiently photolyzing the glyoxal to yield CO. The lamp was therefore exposed for more than 1 h to a 20 Torr sample of glyoxal trapped at liquid nitrogen temperature. Since no CO was detected, it was concluded that trapping effectively removed glyoxal from the cell.

(2) Mixtures consisting of millitorr pressures of CO and torr pressures of glyoxal were prepared to model a typical photolysis reaction. Exposure to liquid nitrogen trapping followed by analysis for CO via resonance fluorescence demonstrated that the initial CO pressure had remained constant while the glyoxal was completely removed.

The potential interference of companion photolysis products such as formaldehyde and molecular hydrogen was also examined. Liquid nitrogen trapping removes formaldehyde to the same degree as glyoxal. Molecular hydrogen, of course, remains in the photolysis cell. A calibration experiment demonstrated that over a wide range of reasonable CO/H_2 pressures, H_2 made no discernable contribution either to enhancing or spoiling CO resonance emission. Over a particular CO concentration range (*e.g.* 5 - 25 mTorr) calibration curves with and without H_2 could not be distinguished from one another.

2.2. Single vibronic level (SVL) populations

The number of glyoxal molecules in a specific SVL was obtained by measuring the total number of photons for the entire photolysis and the absorption coefficient of glyoxal at the photolyzing wavelength. The first data were obtained by monitoring the laser energy per pulse with calibrated

† Focused outputs from lasers of this type are efficient in generating two-photon absorptions [11]. This is not the case in the experiments reported here since the laser output remained unfocused. The data in Fig. 6 confirm this conclusion. Band contours obtained using the unfocused laser as an excitation source (α measurements) compare very well with contours obtained by conventional single-photon absorption spectroscopy.

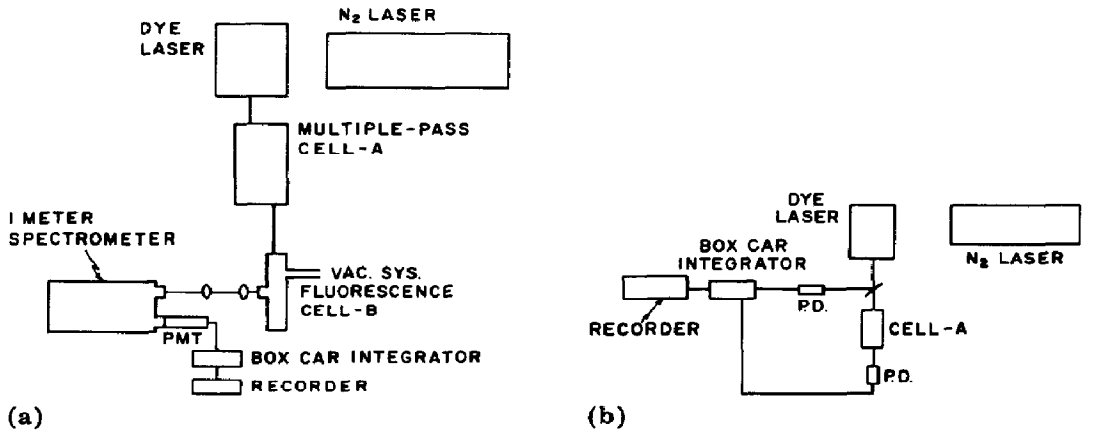

Fig. 3. Experimental apparatus for measuring absorption coefficients: (a) SVL fluorescence method; (b) calibrated photodiode method. See text for detailed descriptions.

photodiodes†, the pulse rate (10 pulses s^{-1}) and the total time for the photolysis. The absorption coefficients were measured by two complementary but separate techniques (Fig. 3). Both use the tuned (0.01 nm FWHM) dye laser output as an excitation source. The absolute wavelength of the dye laser was measured with a 1 m spectrometer working in the second order. Changes in laser intensity resulting from glyoxal absorption were measured by either (1) direct absorption with two photodiodes or (2) SVL fluorescence as detected by an S20 photomultiplier. Both techniques used boxcar integration to analyze the detector's signal.

In the first method (Fig. 3(b)) part of the laser output was reflected by an uncoated pellicle to a photodiode to monitor I_0. The remaining laser radiation passed through a 10 cm cell and onto the photodiode. Glyoxal pressures were measured in the cell with a capacitance manometer (Datametrics Model 570A-10T) to vary I. The ratio of the two photodiode signals (I/I_0) was obtained directly from a dual channel boxcar integrator (PARC Model 162/163) as an A/B output.

The second method used glyoxal fluorescence to measure changes in the laser intensity. Fluorescence to separate vibronic levels in the ground state is one of the processes which relax glyoxal following SVL excitation. Since these transitions originate in a specific excited state vibronic level and terminate in their ground state counterparts, the wavelength-resolved fluorescence spectrum consists of discrete bands which in general are well separated (Fig. 4). The intensity of fluorescence contained in such a spectrum depends on (1) the glyoxal pressure of the fluorescing sample, (2) the wavelength of excitation and (3) the intensity of the laser excitation. If the first two parameters are held constant, then the intensity of fluorescence becomes a function of the laser intensity alone.

† Two different photodiodes with different calibration curves gave the same results.

In our apparatus the laser excitation passed through a multiple-pass cell (cell A in Fig. 3(a)) prior to entering the fluorescence cell (cell B in Fig. 3(a)). The glyoxal pressure in cell B was held constant. The dye laser was tuned into resonance with the SVL used to measure ϕ(CO). The fluorescence from cell B was collected and focused into a 1 m spectrometer and onto the face of a photomultiplier (EMI Model 9659QB). The signal was read on one channel of the boxcar integrator. As the spectrometer was scanned, an SVL fluorescence spectrum such as the one shown in Fig. 4 was generated†. A single fluorescence band (*e.g.* $8_0^1\ 4_1^0$ in Fig. 4) was selected to monitor the

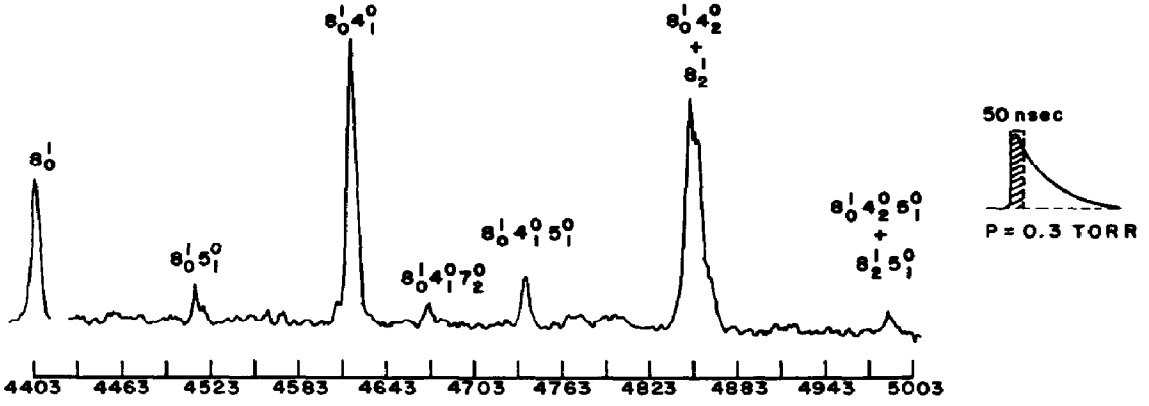

Fig. 4. Time-resolved single vibronic level (TRSVL) fluorescence spectrum. The fluorescence from a 300 mTorr sample of glyoxal following direct population of the 8^1 vibronic level (^1A_u electronic state) is presented with both wavelength and time resolution. The wavelength resolution of the fluorescence is obtained with a 1 m spectrometer. A 50 ns gate set by a boxcar integrator to appear concurrently with the laser excitation (10 ns) generates a TRSVL spectrum containing only transitions from the initially populated vibronic level (*i.e.* 8^1). The vibronic assignments shown refer to the fundamental vibrational modes of glyoxal [13].

relative intensity of glyoxal fluorescence. The area under the band was measured with a planimeter for each change in fluorescence intensity. By filling cell A with varying pressures of glyoxal, the laser intensity entering cell B, and therefore the fluorescence leaving it, was controlled by means of the absorptivity of glyoxal at that specific wavelength. The relative intensity of the fluorescence band thereby became a very sensitive measure of glyoxal absorption coefficient at a specific laser wavelength. The technique is at least an order of magnitude more sensitive to changes in laser intensities than the photodiode method and therefore can be used for very low pressure samples and/or for bands with very small absorption coefficients.

† The 8_0^1, for example, notation describes a transition from the zero point level of the ^1A_g electronic state to one quantum of ν_8 in the ^1A_u electronic state of glyoxal.

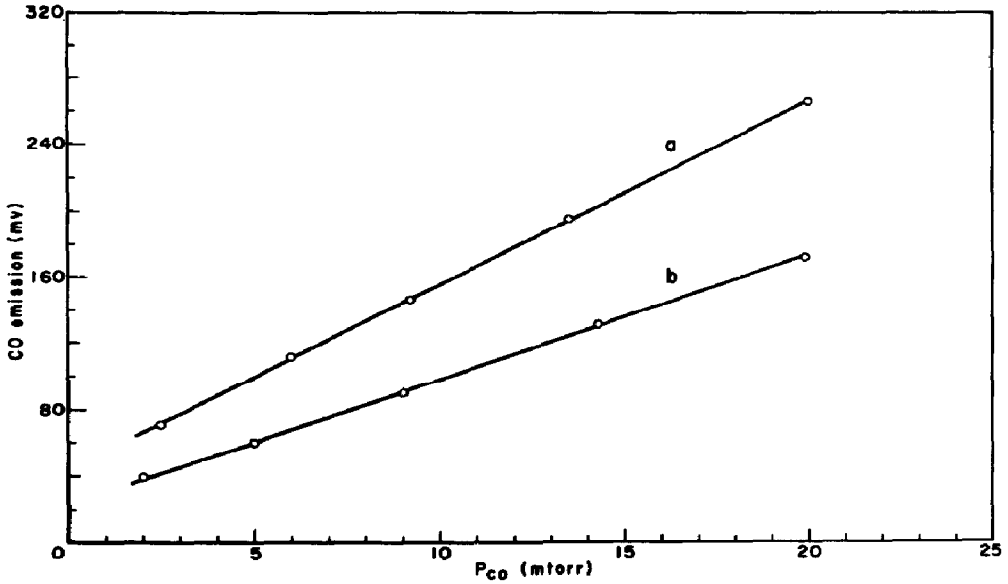

Fig. 5. CO calibration curves. The resonance emission signal from CO as measured by the detection system shown in Figs. 1 and 2 is plotted *vs.* the absolute pressures of CO measured in the reaction cell by a capacitance manometer. Line a is for a newly filled xenon resonance lamp and line b was obtained with a lamp which had been operated for about 100 h.

3. Results

3.1. CO calibration

The resonance emission signal was calibrated against CO pressures measured into the photolysis cell with a capacitance manometer. Figure 5 contains two CO calibration curves taken several days apart. Since it is clear that the slope of this plot depends on the age of the lamp, a CO calibration curve was taken immediately before or after each photolysis experiment. The total pressure of CO generated in photolysis was kept in the 5 - 20 mTorr range which was in the linear part of the calibration curve and well above the 0.5 mTorr limit for quantitative detection with this lamp design.

3.2. Excited state populations

Since the vibronic band contours in glyoxal are approximately 1.0 nm wide, the 0.01 nm bandwidth of the laser output can be easily used to populate a separate vibronic level. The bandwidth, however, is large enough to populate a distribution of rotational levels encompassing a range of rotational quantum numbers. One can infer this directly from the data presented in Fig. 6 and from the rotational analysis of Paldus and Ramsay [12]. In these measurements this distribution remained unknown but constant for each excitation wavelength. The absorption coefficients (α, base 10) for excitation into four such vibronic levels were measured by both techniques described here and the results are presented in Table 1. The

glyoxal pressures used are the same as those used in the photolysis experiments. The results from the two techniques are clearly in excellent agreement (less than 5% variation).

The accuracy of these measurements also can be judged by another aspect of the data presented in Fig. 6. Absorption coefficients were obtained

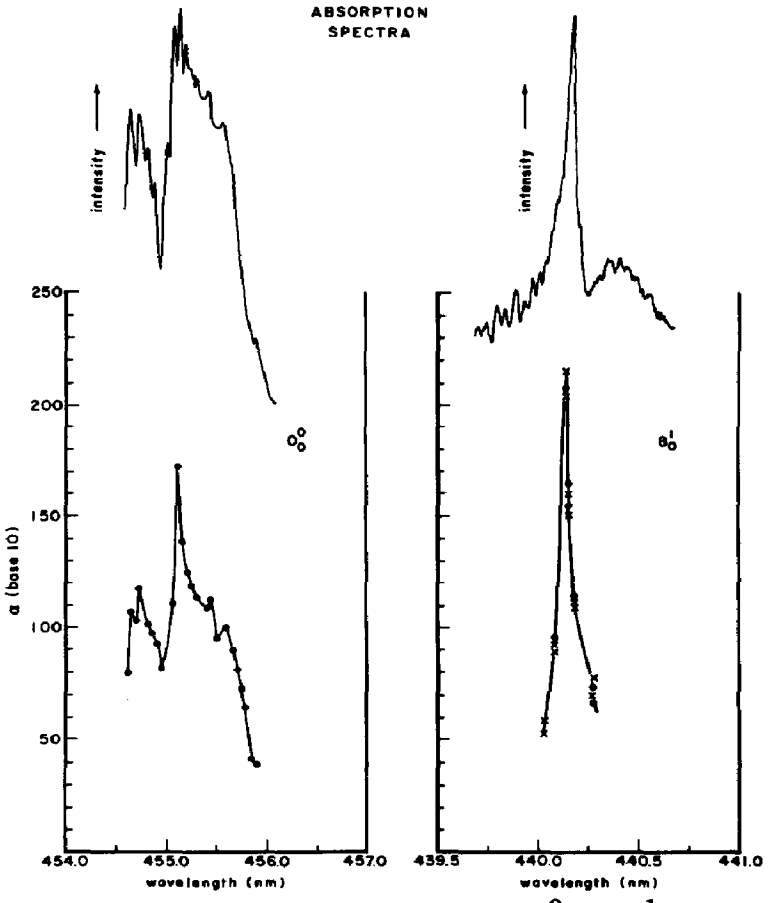

Fig. 6. Absorption band contours for the 0_0^0 and 8_0^1 transitions. Photoelectrically detected absorption band contours for the 0_0^0 and 8_0^1 transitions are shown at the top of the figure. Plots of the absorption coefficients for each band *vs.* wavelength are shown at the bottom. Data points obtained with both the photodiode (•) and SVL fluorescence (×) methods are plotted together for 8_0^1. Data obtained by the photodiode technique only are presented for the 0_0^0 band. The wavelength scales for both plots are aligned without consideration of the spectral features. The left-hand α scale applies to both the 0_0^0 and 8_0^1 bands and the wavelength scales at the bottom of each plot correlate with the band contours obtained from both the photoelectric spectra and the values of α.

as a function of wavelength within the 8_0^1 and 0_0^0 vibronic bands and were compared with the photoelectrically measured absorption contours. The wavelength of the laser was selected for each α determination by a spectrometer. The wavelength scale obtained for the plot of α was then aligned with the wavelength scale of the photoelectric absorption spectrum, independent

TABLE 1

Absorption coefficients α (base 10) for the excitation of glyoxal to several single vibronic levels

Method	Pressure in cell A[a] (Torr)	$^1A_u - ^1A_g$ vibronic transition (wavelength (nm))			
		0_0^0(454.99)	7_1^1(452.65)	5_0^1(444.64)	8_0^1(440.15)
Photodiode	2.7	–	–	–	157
	4.7	127	54.9	31.8	166
	6.6	128	52.8	30.6	166
	8.0	129	51.2	32.1	157
	10.6	124	52.4	31.4	162
Average		127	52.8	31.5	162
SVL	2.7	132	–	33.8	170
Fluorescence	4.7	130	48.3	31.0	152
	6.6	–	50.1	32.3	–
	8.0	–	53.8	31.6	–
	10.6	–	54.0	32.8	–
Average		131	51.6	32.3	161

Values were measured by both the photodiode and SVL fluorescence techniques described in the text. The glyoxal pressures cover the same range used in ϕ(CO) measurements.
[a] Refer to Fig. 3.

of any features in the band contour. The fact that the resulting band contours mirror one another (see Fig. 6) is therefore firm evidence supporting the accuracy of both the absolute wavelengths used in α measurements and the relative α values themselves.

Further confidence in the precision of α values derives from their reproducibility at a given wavelength and pressure. For example, four completely separate experiments using the two techniques described here measured α values at 440.15 nm (8_0^1 band, Fig. 6) which agree to within ±5%.

3.3. ϕ(CO)

We can obtain an indication of the precision of the combined experimental technique from the values of ϕ(CO) themselves. Data for excitation into the 0_0^0 transition of glyoxal at 455.15 nm are shown in Fig.7 as a function of glyoxal pressure. Vertical bars indicating ±5% error are included in order to demonstrate that the measurement is at least that precise.

4. Discussion

The precision, and therefore the usefulness, of absolute quantum yields derives from the precision of their composite measurements, namely the concentration of products, the absorption coefficients and the wavelength

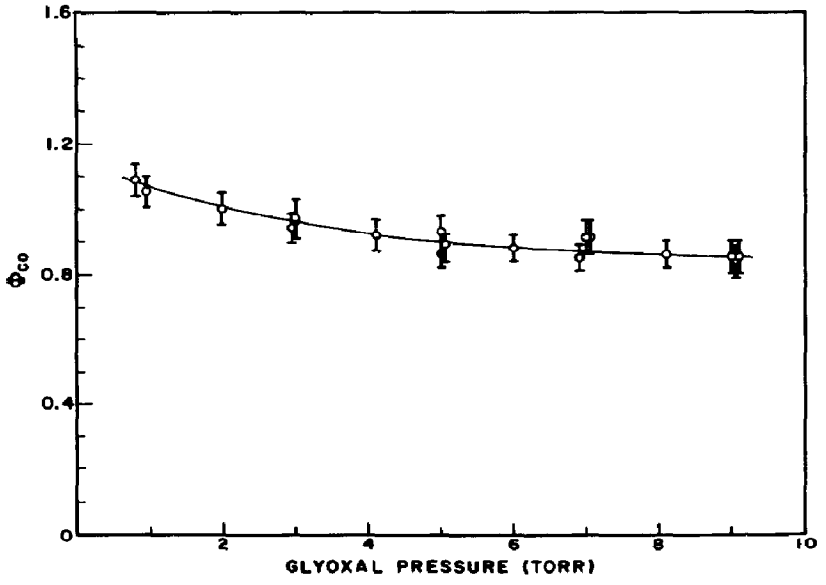

Fig. 7. Absolute quantum yield of CO (ϕ(CO)) following excitation at 455.15 nm within the 0_0^0 vibronic band. ϕ(CO) is plotted *vs.* the total pressure of glyoxal. Vertical bars indicating ±5% errors are included. Two coincident data points are represented by the solid circle near 5 Torr.

correlation between them. The precision of the reported techniques in obtaining these data is established by the results presented in Figs. 5, 6 and 7 and Table 1.

The calibration curves (Fig. 5) demonstrate that VUV resonance emission generated by microwave discharge can quantitatively monitor CO concentrations of the millitorr level with errors of less than 1%. Values for absorption coefficients (Table 1) obtained by the two complementary techniques described here agree to within less than 5%. This result is especially important in view of the extreme rapidity with which the absorptivity of glyoxal changes over the narrow excitation bandwidth defined by the laser. Rovibronic excitation can therefore be used in photolysis without sacrificing accurate measurements of excited state populations. The reproducibility of the narrow 8_0^1 band contour by the plot of α (Fig. 6) clearly indicates that any wavelength calibration errors arising in either photolysis or absorption coefficient measurements originate from the finite bandwidth of the laser radiation and not from the wavelength calibration methods themselves. The 0.01 nm laser bandwidth results in some averaging which appears as a smoothing of the 0_0^0 band contour formed by α values (Fig. 6). The combined precision for all of these measurements is well represented by the values of ϕ(CO) shown in Fig. 7.

The techniques described here for measuring absolute product quantum yields clearly can be applied to products other than CO and to parent molecules other than glyoxal. Many of the advantages and disadvantages of these methods for general applications can be derived from this work.

4.1. Product concentrations

(a) Microwave powered resonance lamps are very versatile excitation sources because they generally use the species to be monitored in the construction of the lamp itself. As long as the atom or molecule undergoes resonance emission in a microwave discharge, it is potentially feasible for it to be monitored. Research in the area of reaction kinetics has led to the development of many VUV resonance lamps capable of detecting a wide range of both stable and reactive species [9]. These lamps are not designed to remain stable over very long periods of time, however, and therefore require the type of stabilization described here before they can be used for product yield analysis.

(b) Since the lamp is tailored to monitor a particular atom or molecule, it is specific for one component in a multicomponent system such as that created in dissociation reactions.

(c) VUV resonance emission is very sensitive. Depending on the species, concentrations below 10^{10} molecules cm^{-3} can be detected (about 10^{14} molecules cm^{-3} were monitored in this work). Since most sensitivity measurements have been made under conditions which involve less lamp stability than required for product yields, these limits must be used only as guidelines. The results obtained with CO in this work indicate that although some sensitivity is lost through lamp stabilization, it remains more than sensitive enough to monitor products in the millitorr pressure regime.

(d) It is a direct physical measurement of concentration. It involves none of the potentially serious problems associated with the use of secondary chemical reactions to analyze for products (*e.g.* chemiluminescence or conversion to secondary products). In addition, errors arising from sampling and manipulation of products prior to analysis are eliminated since detection occurs in the reaction cell.

(e) The photoelectric detection devices available in the VUV are very efficient. This contributes directly to the detection sensitivity. The use of VUV radiation is also the basis, however, for the most serious disadvantage of the technique: lamp photolysis. The very efficient photolysis of the parent as well as some dissociation products (*e.g.* H_2CO) requires that some separation of the photolysis mixture be carried out prior to analysis. In many instances low temperature trapping appears to be a practical solution to this problem.

4.2. Absorption coefficients

(a) The use of the photolysis laser as an excitation source in α measurements eliminates errors stemming from differences in spectral resolution, absolute wavelength and bandwidths. The α values are measured using precisely the same spectral conditions as the photolysis.

(b) The photodiode technique is simpler than SVL fluorescence but less sensitive to changes in the transmission (ΔT) of the sample arising from absorptions. SVL fluorescence was capable in this work of observing at least an order of magnitude smaller ΔT values. Integration of larger areas and/or

longer accumulation time are experimental parameters which should further increase this sensitivity. When combined with a multiple-pass absorption cell, SVL fluorescence is clearly the method of choice for weakly absorbing systems.

5. Summarizing remarks

The results presented here have demonstrated that absolute product quantum yields can be obtained even under the stringent conditions associated with rovibronic excitation in low pressure gas phase samples. The experimental techniques for measuring product concentrations and absorption coefficients can be applied with some modifications to a variety of specific dissociation reactions other than the production of CO from glyoxal. This type of data contains important aspects of the detailed information required to evaluate the feasibility of selected-state excitation for the control of dissociative reactions.

Acknowledgments

The authors wish to thank Dr. Louis Stief and the National Aeronautics and Space Administration for the temporary use of microwave equipment, Mr. Robert Malstrom for help in the preparation of Fig. 6 and Dr. M. Sage for the use of recording equipment. GHA also wishes gratefully to acknowledge support for this research from the U.S. Army Research Office — Durham, under Grant DAAG29-75-G-0104, the Petroleum Research Fund of the American Chemical Society and the Research Corporation. CGV wishes to thank the Syracuse University Senate Research Fund for partial support.

References

1 J. C. Hemminger and E. K. C. Lee, J. Chem. Phys., 54 (1971) 1405.
2 E. S. Yeung and C. B. Moore, J. Chem. Phys., 58 (1973) 3988.
3 J. R. McDonald and L. E. Brus, Chem. Phys. Lett., 7 (1972) 247.
4 C. A. Thayer and J. T. Yardley, J. Chem. Phys., 57 (1972) 3992.
5 K. Y. Tang and E. K. C. Lee, J. Phys. Chem., 80 (1976) 1833.
6 G. H. Atkinson, M. E. McIlwain and C. G. Venkatesh, J. Chem. Phys., 68 (1978) 726.
7 R. Gorden, Jr., R. E. Rebbert and P. Ausloos, Nat. Bur. Stand. (U.S.), Tech. Note 496 (1969).
8 See for example T. G. Slanger and G. Black, J. Chem. Phys., 51 (1969) 4534.
9 See for example D. Davis and W. Braun, Appl. Optics, 7 (1968) 2071.
W. Braun and T. Carrington, J. Quant. Spectrosc. Radiat. Transfer, 9 (1969) 1133.
10 See for example H. Okabe, J. Opt. Soc. Am., 54 (1964) 478.
J. R. McNesby and H. Okabe, Adv. Photochem., 3 (1965) 157.
11 See for example R. M. Hochstrasser, H.-N. Sung and J. E. Wessel, J. Am. Chem. Soc., 95 (1973) 8179.
12 J. Paldus and D. A. Ramsay, Can. J. Phys., 45 (1967) 1389.
13 E. Photos and G. H. Atkinson, Chem. Phys. Lett., 36 (1975) 34.